Flow Around Bodies

Underlying Flow Regime 2-02

Table of Contents

UNDERLYING FLOW REGIME 2-02 1

DESCRIPTION 2

PREFACE 2
INTRODUCTION 3
REVIEW OF UFR STUDIES AND CHOICE OF TEST CASE 3

TEST CASE 5

BRIEF DESCRIPTION OF THE STUDY TEST CASE 5
TEST CASE EXPERIMENTS 5
CFD METHODS 7

COMPARISON OF CFD CALCULATIONS WITH EXPERIMENTS 10

BEST PRACTICE ADVICE FOR THE UFR 16

KEY PHYSICS 16
NUMERICAL ISSUES 16
COMPUTATIONAL DOMAIN AND BOUNDARY CONDITIONS 17
PHYSICAL MODELLING 17
APPLICATION UNCERTAINTIES 18
RECOMMENDATIONS FOR FUTURE WORK 18

REFERENCES 19

Abstract

The flow past cylinders is an important flow type that occurs in many engineering applications. Although it was detected in only one application challenge (namely in AC4-06), cylindrical structures exposed to flow are basically present in all areas of engineering and in the environment. Often the flow is associated with unsteady vortex shedding and this special feature has a dominant influence on the flow behaviour itself, on the loading of cylindrical structures which is often unsteady and on heat transfer. A wide variety of configurations is possible ranging from infinitely long cylinders in uniform flow normal to the cylinder to cylinders placed in sheared flow like in boundary layers, cylinders at angles to the flow, prismatic or tapered cylinders, various cross-sectional

geometries, cylinders having short aspect ratios etc. etc. Here, attention is restricted to infinitely long, prismatic cylinders placed normal to uniform flow and only cylinders with circular and square cross sections are considered; the actual study test case will be the flow around a square cylinder.

The flow past long cylinders exposed to uniform approach flow is an interesting and important test case for CFD calculations because the geometry is simple, but the flow is complex with a rich variety of phenomena occurring. These include thin, separating shear layers, alternating shedding of vortices from the cylinder which are transported downstream, where they retain their identity in a Karman vortex street for a considerable distance, but are eventually broken up and diffused by the turbulent motion. These vortices are predominantly two-dimensional and so is the time- mean flow, but large–scale 3-D structures exist which lead to a modulation of the shedding frequency. The shedding causes unsteady forces on the cylinder which may lead to flow induced vibrations. The approach stagnation flow is basically inviscid and thin laminar boundary layers are formed on the forward faces of the cylinder. The cylinder may have various geometries, but the circular and square shape are the most common ones and will only be considered further. In the case of the square cylinder, the flow separates at the front edges and a flapping shear layer develops on the sides of the cylinder, which is initially laminar but becomes turbulent fairly quickly when the Reynolds number is above 600. In this range, the drag coefficient and dimensionless shedding frequency (Strouhal number) do not depend much on the Reynolds number. In the case of the circular cylinder, the separation point is not fixed but depends on the boundary layer development before separation, which depends on the Reynolds number. For $Re > 300$ the wake of the cylinder is turbulent and when $Re < 1.5 \times 10^5$ the boundary layer remains laminar up to separation. This is called the subcritical region in which the drag coefficient increases with Reynolds number while the Strouhal number is fairly constant. For $1.5 \times 10^5 < Re < 3.5 \times 10^6$ the boundary layer on the cylinder becomes turbulent before separation which thereby moves backwards, the drag is reduced significantly (drag crisis) and the Strouhal number is increased. This is called the transitional region. For $Re > 3.5 \times 10^6$ the boundary layer on the cylinder is largly turbulent and the strong Reynolds number dependence of drag coefficient and Strouhal number ceases. This is called the super-critical region. Because of the overruling influence of the unsteady vortex shedding, CFD calculations need to be unsteady.

Description

Preface

The flow past cylinders is an important flow type that occurs in many engineering applications. Although it was detected in only one application challenge (namely in AC4-06), cylindrical structures exposed to flow are basically present in all areas of engineering and in the environment. Often the flow is associated with unsteady vortex shedding and this special feature has a dominant influence on the flow behaviour itself,

on the loading of cylindrical structures which is often unsteady and on heat transfer. A wide variety of configurations is possible ranging from infinitely long cylinders in uniform flow normal to the cylinder to cylinders placed in sheared flow like in boundary layers, cylinders at angles to the flow, prismatic or tapered cylinders, various cross-sectional geometries, cylinders having short aspect ratios etc. etc. Here, attention is restricted to infinitely long, prismatic cylinders placed normal to uniform flow and only cylinders with circular and square cross sections are considered; the actual study test case will be the flow around a square cylinder.

Introduction

The flow past long cylinders exposed to uniform approach flow is an interesting and important test case for CFD calculations because the geometry is simple, but the flow is complex with a rich variety of phenomena occurring. These include thin, separating shear layers, alternating shedding of vortices from the cylinder which are transported downstream, where they retain their identity in a Karman vortex street for a considerable distance, but are eventually broken up and diffused by the turbulent motion. These vortices are predominantly two-dimensional and so is the time- mean flow, but large–scale 3-D structures exist which lead to a modulation of the shedding frequency. The shedding causes unsteady forces on the cylinder which may lead to flow induced vibrations. The approach stagnation flow is basically inviscid and thin laminar boundary layers are formed on the forward faces of the cylinder. The cylinder may have various geometries, but the circular and square shape are the most common ones and will only be considered further. In the case of the square cylinder, the flow separates at the front edges and a flapping shear layer develops on the sides of the cylinder, which is initially laminar but becomes turbulent fairly quickly when the Reynolds number is above 600. In this range, the drag coefficient and dimensionless shedding frequency (Strouhal number) do not depend much on the Reynolds number. In the case of the circular cylinder, the separation point is not fixed but depends on the boundary layer development before separation, which depends on the Reynolds number. For $Re > 300$ the wake of the cylinder is turbulent and when $Re < 1.5 \cdot 10^5$ the boundary layer remains laminar up to separation. This is called the subcritical region in which the drag coefficient increases with Reynolds number while the Strouhal number is fairly constant. For $1.5 \cdot 10^5 < Re < 3.5 \cdot 10^6$ the boundary layer on the cylinder becomes turbulent before separation which thereby moves backwards, the drag is reduced significantly (drag crisis) and the Strouhal number is increased. This is called the transitional region. For $Re > 3.5 \cdot 10^6$ the boundary layer on the cylinder is largly turbulent and the strong Reynolds number dependence of drag coefficient and Strouhal number ceases. This is called the super-critical region. Because of the overruling influence of the unsteady vortex shedding, CFD calculations need to be unsteady.

Review of UFR studies and choice of test case

There have been numerous experimental studies of the flow past circular cylinders, covering a wide range of Reynolds numbers, and the book of Zdravkovich (1997) gives a good overview of the findings. However, in most experiments only global parameters

like drag coefficient and Strouhal number were measured and not the details of the flow development. The only detailed phase-resolved measurements of the flow past a circular cylinder were carried out by Cantwell and Coles (1983) at Re = 140.000. The data is available on the CD of the AGARD-AR-345-report (1998). Attempts to calculate this flow with RANS models in unsteady calculations (i.e. basically URANS calculations) were not very successful. LES calculations clearly yielded superior results but also gave rise to some problems for this case, presumably because it was close to the critical Reynolds number. Extensive calculations have been done for a lower Reynolds number of Re = 3.900 with LES but also DNS. The simulations for the two Reynolds numbers are reviewed in Rodi (2002) and LES results for the Re = 3.900 case can be found in the FLOWNET data base.

For the flow past a square cylinder, there are considerably fewer experimental studies then for the flow past the circular one. A brief review is given in the AGARD-AR-345 report. The only experiment with phase–resolved results is that due to Lyn and Rodi (1994) and Lyn et al. (1995) who provided detailed measurements of the flow past a square cylinder at Re = 22.000 obtained with a laser Doppler velocimeter. This flow has been calculated with a wide variety of RANS models (2 D unsteady calculations) and has been used as test case at two LES workshops (Rodi et al. 1995, 1997, Voke 1997), so that numerous LES results are available. Also after the workshops, this flow has been used as test case for LES simulations over and over again. Further, review articles exist summarizing the RANS and LES simulations available (Rodi 1997, 2002) and for all these reasons this flow was chosen as the UFR study test case. Another reason for the choice is that the experiment was carried out in the group of the present author which also performed calculations and hence the experiment was clearly designed for CFD validation.

Test Case

Brief description of the study test case

The case considered is the flow past a square cylinder at Re = UD/v = 22.000, as sketched in Fig.1. The approach flow is uniform (velocity U) and the free stream is confined by two sidewalls (the walls of the water tunnel), the blockage by the cylinder being 7.1 %. In the experiment, the cylinder had of course a finite length (of about 10 D) and was confined by the bottom and top wall of the water tunnel, but here the end effects are not considered and the case of an infinitely long cylinder is taken.

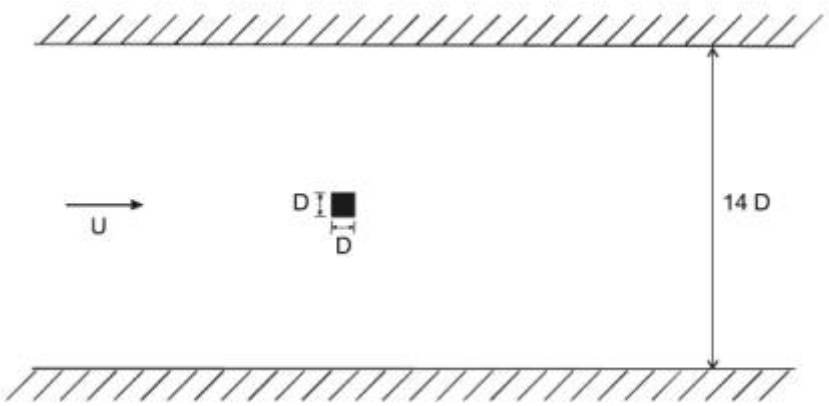

Figure 1: Flow geometry

The principal measured quantities which should be used for an assessment of CFD calculations are as follows:

- Strouhal number St = fD/U, which is the shedding frequency of the vortices f, made dimensionless.
- Mean drag coefficient C_D
- RMS of fluctuating drag coefficient, C_D', and of fluctuating lift coefficient C_L'
- distribution of mean pressure around cylinder faces
- length of mean recirculation region behind cylinder, L_R
- distribution of mean velocity U_{CL} along centre line of cylinder
- distribution of kinetic energy of total (periodic and stochastic) fluctuations, k_{total} , along centre line of the cylinder.

For a more detailed test of the CFD calculations, the distributions of averaged streamwise and transverse velocity as well as turbulent normal and shear stresses in the vicinity of the wake can be taken either in form of contour plots or profiles at various downstream cross sections. Time-mean averages over all phases are of interest here and for a detailed study of the time-dependent behaviour also phase average values at various phase angles during the period of the vortex shedding.

Test Case Experiments

The experiments are described in detail in Lyn and Rodi (1994) and Lyn et al. (1995). The cylinder was 40 mm in width and 392 mm long mounted in the rectangular test section of a water channel 392 mm x 560 mm (blockage 7.1 %). The free stream

approach velocity U was approximately 0.54 m/s yielding a Reynolds number Re = UD/v = 22.000. At this Reynolds number the flow is approximately periodic with a Strouhal number St of 0.133 ± 0.004. The approach flow had a turbulence level of about 2 %. The velocity measurements were made above the upper surface and behind the cylinder up to 8 diameters downstream. The measurements were taken with a single component laser Doppler Velocimeter (LDV) just above the upper surface of the cylinder and a two component LDV in the other regions — the locations of the measurement points are given in Fig. 2. Bragg cells were employed to provide an offset frequency necessary to capture the reversal of flow direction in regions of separation. A low-pass filtered pressure signal from a tap on the cylinder side-wall was used to obtain a reference phase for phase-averaging the velocity measurements. 20 phase bins were used for phase-averaging.

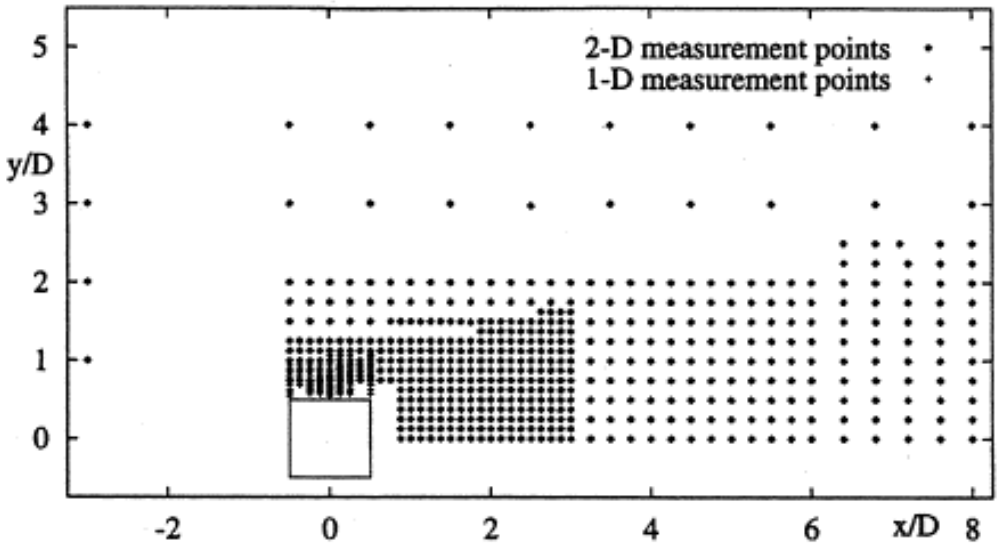

Figure 2: Coordinate system and location of measurement points

The quantities measured at the points given in Figure 2 are the following:

- average streamwise flow velocity, U_1
- average transverse flow velocity, U_2
- average normal stresses, $\overline{u_1 u_1}$, $\overline{u_2 u_2}$
- average turbulent stress, $\overline{u_1 u_2}$

The Strouhal number was determined from the fluctuating pressure signal mentioned above as

St = 0.133 ± 0.004 .The drag was not measured directly, but the mean drag coefficient was determined from the velocity distribution in the wake to be $C_D \approx 2.1$.

The pressure distribution along the cylinder walls has not been measured in these experiments. Here the measurements of other authors performed under similar conditions must be consulted (e.g. Bearman and Obajasu 1982).

The measurement uncertainties are:

U_1 and U_2 : 5% of approach velocity

$\overline{u_1 u_1}$, $\overline{u_2 u_2}$

$\overline{u_1 u_2}$: 15% to 25% .

The measured mean velocity along the centre line approaches the free stream velocity rather slowly, see Fig. 3 below. Most calculations yielded a considerably faster recovery of the centre line velocity and hence some doubts were voiced concerning the reliability of the measurements. However, independent measurements of Martinuzzi and Wu (1997) under similar conditions (blockage and turbulence level of the approach flow) yielded very similar results and give credibility to the measurements of Lyn et al. (1995).

The boundary layers on the top and bottom walls where the cylinder was mounted were fairly thin so that the end effects were small. The flow at the mid height of the cylinder where the measurements were taken corresponds closely to the flow past an infinitely long cylinder. The conditions on the boundaries of the flow are well known. They are no-slip conditions on the cylinder walls and on the side walls of the tunnel, but since the boundary layers on the latter were thin these can be considered as frictionless walls. The approach flow was measured 3 cylinder widths upstream and had a turbulence level of about 2% and a centre-line mean velocity deficit of about 5 to 10%. If uniform inflow conditions are to be used in calculations, the inflow boundary should be placed further upstream (5 to 10 D). The intensity of the approach-flow fluctuations is known from the measurements to be about 2% but no information is available from the measurements on the length scale of the turbulence. In RANS calculations this was estimated by assuming a ratio of eddy viscosity to molecular viscosity in the range 10 to 100, and Bosch and Rodi (1998) found that the value of 10 is more suitable for this case.

The measurement data are available both in the ERCOFTAC database Test Case 43 and on the CD of the AGARD-AR-345-report.

CFD Methods

The study test case was calculated with a large number of RANS and LES methods. In the RANS calculations, 2D unsteady equations were solved thereby attempting to resolve the periodic fluctuating motion and to simulate the superimposed stochastic turbulent motion by a RANS turbulence model so that the calculations were really URANS. A wide variety of turbulence models was used, ranging from the algebraic Baldwin-Lomax model to a Reynolds stress model (RSM).

The most extensive testing was done with variants of the k-ε model and is reported in Rodi (1997) and Bosch and Rodi (1998) -and also reviewed in these papers. Algebraic stress models have also have been applied on this flow (Lakehal et al. 1998). Since the standard k-ε model is known to produce excessive turbulence production in stagnation regions, the Kato-Launder (1993) modification was also tested which suppresses this excessive production. Various near-wall treatments were applied in connection with the different RANS models such as the use of standard wall functions bridging the viscous sublayer but also two-layer approaches in which the basic turbulence model was only used outside the viscous sublayer while this was resolved with a simpler one-equation

model. The numerical grids used there were of the order of 100 x 70 when wall functions were applied and 170 x 170 when the two-layer approach was used. In preliminary tests it was found out that these grids yielded accurate numerical solutions. The RANS calculations were obtained with various finite-volume codes, some using staggered and some non-staggered grid arrangements. The details are described in the source papers. It is worth noting however that already in the early calculations it was found out that first order upwind difference schemes cannot be used for vortex shedding calculations as they damp out the periodic shedding motion. In the calculations of Bosch and Rodi (1998), the HLPA (hybrid linear parabolic approximation) method of Zhu (1991) was used, which is low-diffusive and oscillation free. Bosch and Rodi investigated the influence of the location of the inflow boundary and the value of the turbulent length scale specified there. They found that a location of the inflow boundary 4.5 D upstream of the cylinder is too close, as the presence of the cylinder is already felt at this location and the boundary should be shifted further upstream to about 10 D. Also they found a significant influence of the specification of the turbulent length scale at inflow on the calculation results. They determined that a length scale based on the assumption of a ratio of eddy to molecular viscosity of 10 to be more realistic than the previously used value of 100.

In the LES calculations, the 3D, time-dependent Navier-Stokes equations were solved and all motions with scale larger than the mesh size were calculated directly. The effect of the unresolved sub-grid scale motion was in most cases accounted for by a sub-grid scale model but in some cases no such model was used and the dissipative effect of the sub-grid stresses was achieved by numerical damping introduced by a third order upwind scheme for the convection terms. Many calculations were carried out with the Smagorinsky eddy-viscosity model, modifying the length scale near the wall by a van Driest damping function. The popular dynamic approach of Germano et al. (1991) has also been used in a number of cases, mostly with the Smagorinsky model as a base so that the approach then determines the spatial and temporal variation of the Smagorinsky "constant" by making use of the information available from the smallest resolved scales. Some calculations were also carried out with a one-equation model as base in which the velocity scale of the subgrid-scale stresses is calculated from a transport equation for the turbulent subgrid-scale energy. Finally, mixed models combining a scale-similarity model based on a double filtering approach with the Smagorinsky model as well as a filtered structure function model have also been applied. For details of the individual models, the sources must be consulted, but Table 1 lists the subgrid-scale model used in the LES calculations summarised there. The table gives also information on the near-wall treatment and in most calculations no slip conditions have been used at the wall, while in a few calculations wall functions were applied, mainly the Werner-Wengle (1989) approach which assumes a distribution for the instantaneous velocity inside the fist grid cell. A wide variety of numerical solution procedures have been employed, and again the sources must be consulted for details which are however summarised also in the proceedings of the various workshops. The discretization used for convection is again listed for the various calculations in Table 1 and it is important to note here that in LES calculations both spatial and temporal

discretization must be at least second order accurate. Usually the numerical grids were stretched in order to achieve a better resolution in the near-wall region with higher gradients; in some cases embedded grids where used to better resolve this region and also semi-structured grids. The schemes are generally explicit with small time steps to resolve the turbulent fluctuations and various time discretization methods were employed —mostly the second order Adams-Bashforth scheme but also the Runge-Kutta, Euler and leap-frog methods. At the outlet, the calculations were all done with the convective conditions. Typical grids used are shown in Table 1. Grid-refinement has generally not been undertaken and it should be noted that LES calculations are not expected to be grid-independent anyway as the subgrid-scale modelling depends an the mesh-size.

The study test case was posed as a test case for an LES workshop held in 1995 at Rottach-Egern, Germany, and nine groups submitted 16 different results that are reported in Rodi et al. (1995) and partly also in a summary paper of Rodi et al. (1997). These calculations were all performed on a computation domain of 4 D in the spanwise direction, extending 4.5 D upstream of the cylinder, 6.5 D on either side of the cylinder (were the tunnel walls were located) and at least 14.5 D downstream of the cylinder. There was a great variety in the results, and hence the same test case was posed again at a workshop held in 1996 in Grenoble, France. The same calculation domain was prescribed and was mostly also used in later calculations. For the Grenoble workshop, seven groups presented 20 results. These are summarized in Voke (1997). Sample results from both workshops are presented and compared in section 6. The full information on both workshops including the results is available in electronic form and will be entered in the Knowledge Base (link will be provided in the final version of this document).

Védy and Voke (2001) studied systematically the influence of resolution in the various directions and to some extent of the size of the computation domain (but not going beyond 4D in the spanwise direction) as well as of the sub-grid scale model.

Comparison of CFD calculations with Experiments

Table 1 summarizes calculation results for various global parameters such as the Strouhal number (dimensionless shedding frequency, the time-mean drag-coefficient C_D, the RMS values of the fluctuations of drag- and lift-coefficients $C_{D'}$ and $C_{L'}$, respectively, and the reattachement length L_R indicating the length of the time-mean separation region behind the cylinder. The table was mainly taken from the review article of Rodi (2002), but some results that became available after the preparation of this article are also included. The experimental values of Lyn et al. (1995) are also included, but for C_D a range covering also other, similar experiments, is given; the value of C_D determined indirectly by Lyn et al. is 2.1. Most LES calculations yielded the correct value of St ≈ 0.13, and it appears that St is not very sensitive to the parameters of the simulation; there are however a few deviations, notably the calculations not using a subgrid-scale model. The mean drag coefficient is also predicted mostly in generally good agreement with the experiments, but there is a tendency of methods using upwind differencing to yield too high values. There is considerable variation in the recirculation length L_R which will be discussed in connection with the center-line velocity distribution in Fig. 3. The fluctuations of the force-coefficients also show fairly large variation. Unfortunately there are no experimental results available for comparison, but $C_{D'} \approx 0.13$ to 0.2 and $C_{L'} \approx 1.2$ to 1.5 appear reasonable.

The Strouhal number is predicted reasonably well also by most RANS models, but the versions using the Kato-Launder (KL) modification and/or the two-layer approach yield to somewhat too high values. The mean drag-coefficient is significantly underpredicted by the standard k-ε model but roughly the correct value was obtained when the KL modification was used with the two-layer approach, and also by algebraic stress models. The RSM gives the correct value of C_D with wall-functions but overpredicts it in the two-layer approach. This result is consistent with the significant overprediction of the length of the recirculation region by the standard k-ε model and its underprediction by the two-layer RSM.

Calculation method			St	C_D	C_D'	C_L'	L_R/D	grid $N_x \times N_y \times N_z$
LES	KAWAMU, No SGS, NS	3rd UW	0.15	2.58	0.27	1.33	1.68	125 x 78 x 20
Rottach-Egern	UMIST2, Dyn, WF	CD	0.09	2.02	-	-	1.21	140 x 81 x 13
Rodi et al	UKAHY2, Smag, WF	CD	0.13	2.30	0.14	1.15	1.46	146 x 146 x 20
(1997)	TAMU2, Dyn, NS/WF	3rd UW	0.14	2.77	0.19	1.79	0.94	165 x 113 x 17
	UK1, Smag, WF	CD	0.13	2.20	0.14	1.01	1.32	109 x 105 x 20
	UK3, Smag, NS	CD	0.13	2.23	0.13	1.02	1.44	146 x 146 x 20
LES	NT7, LDM, WF	CD	0.131	2.05	0.12	1.39	1.39	140 x 103 x 32
Grenoble	UOI, Dyn., NS	5th UW	0.13	2.03[1)]	0.18	1.29	1.20	192 x 160 x 48
Voke	IS3, Dyn. mix, NS	5th UW	0.133	2.79	0.36	1.68	1.36	112 x 104 x 32
(1997)	TIT, Dyn, NS	3rd UW	0.131	2.62	0.23	1.39	1.23	121 x 113 x 127[2)]
	ST5, Smag, NS	variable 3rd UW	0.161	2.78	0.28	1.38	1.02	107 x 103 x 20
LES	Smag, NS		0.126	2.21	0.16	1.47		
Sohankar	Dyn, NS	CD	0.125	2.04	0.20	1.22	≈1.0	185 x 105 x 25
(1998)	OEDSM, NS		0.129	2.25	0.20	1.50		
RANS	Std. k-ε, WF		0.134	1.64	≈ 0	0.305	2.8	100 x 76
Bosch	Kato-Launder k-ε, WF		0.142	1.79	0.012	0.614	2.04	100 x 76
(1995)	Two-layer k-ε		0.137	1.72	≈ 0	0.426	2.4	170 x 170
	Two-layer Kato-Launder k-ε		0.143	2.0	0.07	1.17	1.25	170 x 170
RANS	RMS, WF		0.136	2.15	0.27	1.49	0.98	70 x 64
Franke &	Two-layer RSM		0.159	2.43	0.06	1.3	1.0	186 x 156
Rodi (1993)								
Experiments			0.132	1.9 - 2.2			1.38	
LES B_1	DOEM, NS, struct.	CD	0.130	2.178	0.192	1.474	1.065	1 Mio.
Schmidt B_2	DOEM, NS, semi-struct.	CD	0.137	2.375	0.138	1.544	1.26	1 Mio.
(2000) B_3	Smag, NS, semi-struct.	CD	0.134	2.406	0.194	1.592	1.305	1 Mio.
LES	Filtered							
Giammanco	Structure	3rd UW I	0.133	2.5	0.29	1.58	1.14	197 x 178 x 32
et al. (2001)	Function Model, NS	II	0.13	2.4	0.28	1.47	1.27	
RANS	ASM – CLS		0.135	2.27	0.107	1.53	1.22	
Lakehal	ASM – LCL		0.128	2.18	0.187	1.53	1.22	
et al. (1998)								

Table 1: Global parameters for flow past square cylinder (UW = upwind diff., CD = central differencing, WF = wall function, NS = no slip, 1) = adjusted for different blockage, 2) = outermost mesh with mbedded meshes), above double line: from Rodi (2002), below double line: additional results

Fig. 3 shows the distribution of the time-mean velocity U along the cylinder center-line. Figure parts a) to c) were taken over from the review of Rodi (2002) and present results from the Rottach-Egern and Grenoble workshops and Fig. 3d) presents recent LES results of Schmidt (2000) and Fig. 3e) RANS results from Bosch and Rodi (1998). As was mentioned already, the experimental velocity recovers very slowly in the down-stream region or even seems to level off at a value of about 0.6 of the approch flow value. The LES exhibit a great variance in this region. Most of the calculations predict the recovery considerably faster than the experiments; those which have the slowest recovery deviate more from the experiments near the cylinder as they predict the recirculation length too short. Schmidt and Thiele (2002) present Detached Eddy-

Simulations (DES) in which the Spalart-Allmaras model is used in RANS mode near the wall and in LES mode away from the wall. The results are similar to the LES results of Schmidt (2000) in Fig. 3d), but strangely they seem to improve when the resolution in the spanwise direction is reduced resulting in the limit in a virtually 2D flow field. However, the Strouhal number then is too small and the mean-drag coefficient too large. Giammanco et al. (2001) also get fairly good centre-line velocity distribution with nearly the correct recovery of the velocity but some underprediction of the reverse flow near the cylinder. It is not really clear why these calculations yielded better predictions of the velocity distribution (and also good predictions of the fluctuations); perhaps this has to do with the use of a larger calculation domain upstream of the cylinder (x/D = 6.5) and of smaller mesh-sizes near the wall and hence better resolution there than in other calculations.

The RANS calculations presented in Fig. 3e) all show too fast recovery in the far field. The standard k-ε model with wall-functions predict a significantly too long recirculation, and using the two-layer approach instead of wall-functions reduces the recirculation length. Considerable improvement is obtained with the Kato-Launder (1993) modification, especially when it is combined with the two-layer approach. When the RSM model is combined with this approach, the recirculation length is predicted too short and the recovery of the velocity is considerably too fast.

Fig. 4 presents the distributions of total (periodic plus stochastic) fluctuations along the centre-line and again parts a) and b) were taken from the review of Rodi (2002). Fig. 4a) shows the total resolved fluctuating kinetic energy of LES calculations from the Rottach-Egern workshop. The results show a rather wide variation with an almost 4-fold difference in the peak level of k_{tot}. Fig. 4b) shows the results for the total u' and v' fluctuations from the Grenoble workshop in comparison with Lyn et al.'s (1995) measurements. The variance is now somewhat smaller (a factor of about 2), but none of the calculations is entirely satisfactory. For these quantities, the results of Sohankar et al. (2000) and also those of Giammanco (2001) agree quite well with the experiments. The LES and DES of Schmidt (2000) and Schmidt and Thiele (2002) are also capturing the total kinetic energy distribution rather well. When in the DES the spanwise resolution is reduced strongly and the flow behaviour becomes more 2-dimensional, the streamwise fluctuations are increased considerably while the spanwise fluctuations go towards zero.

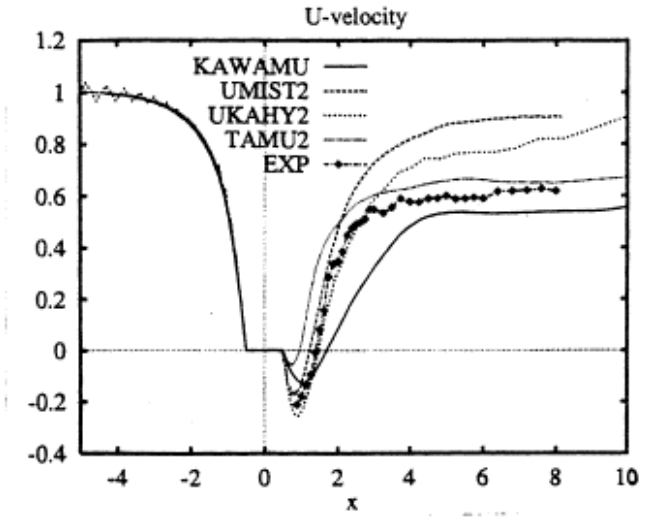

a) Results from Rottach-Egern Workshop (Rodi et al, 1995)

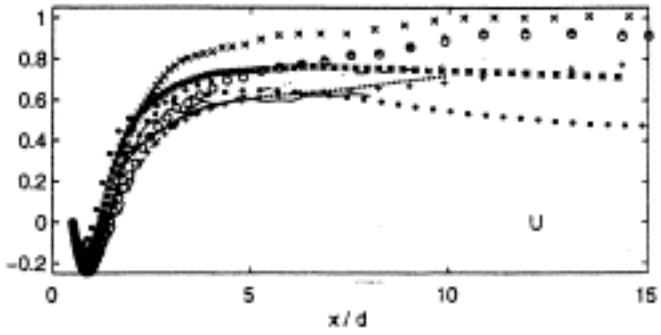

b) Results from Grenoble Workshop - complete wake, — expts., simulations: UK1 o, UK3 O, UOI *, IS3 +, NT7 x, TIT •, ST5 • (from Voke, 1997)

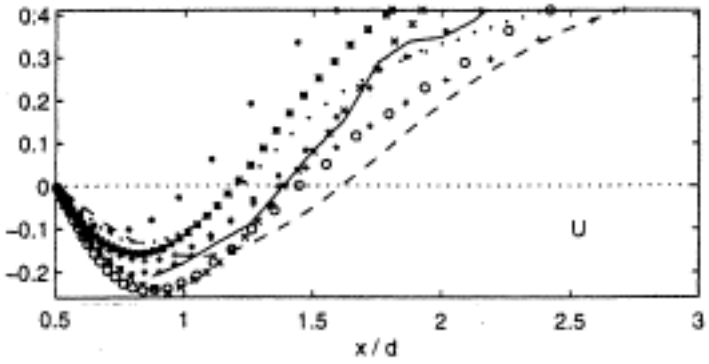

c) Results from Grenoble Workshop - near wake; key as Fig. 3b (from Voke, 1997)

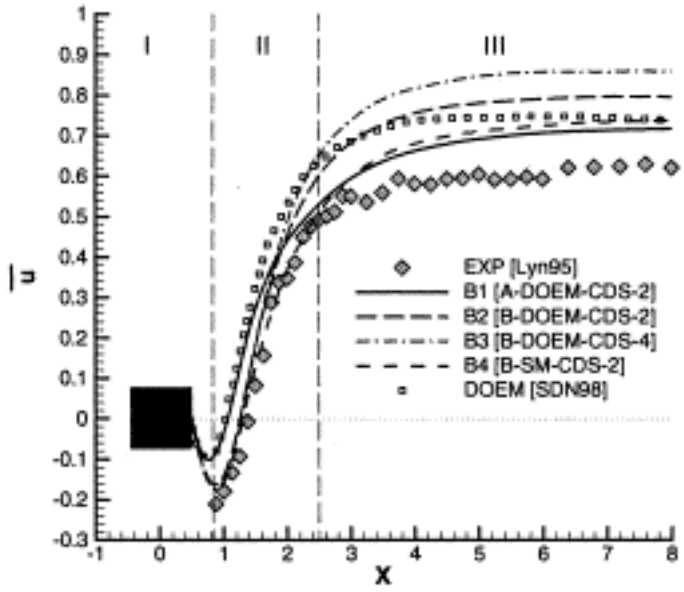

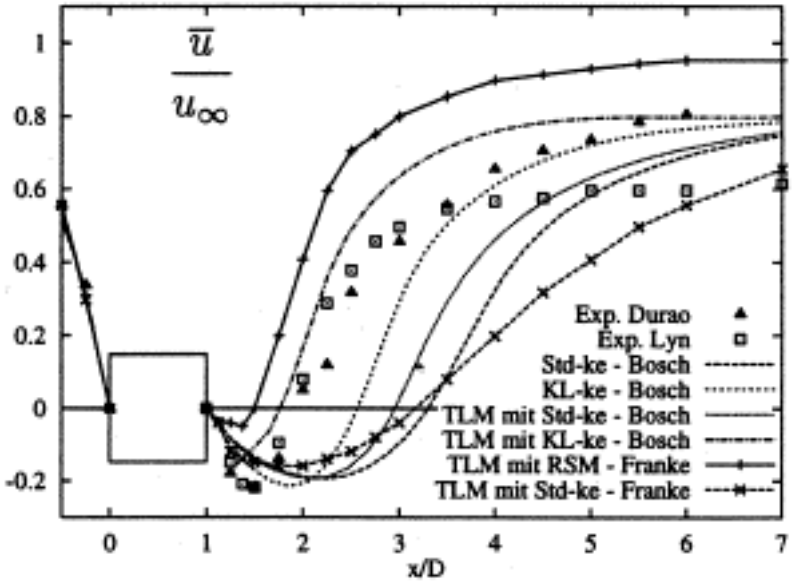

d) LES-results from Schmidt (2000) e) RANS results from Bosch and Rodi (1998)
Figure 3: Time-mean velocity U/U∞ along centre-line of square cylinder

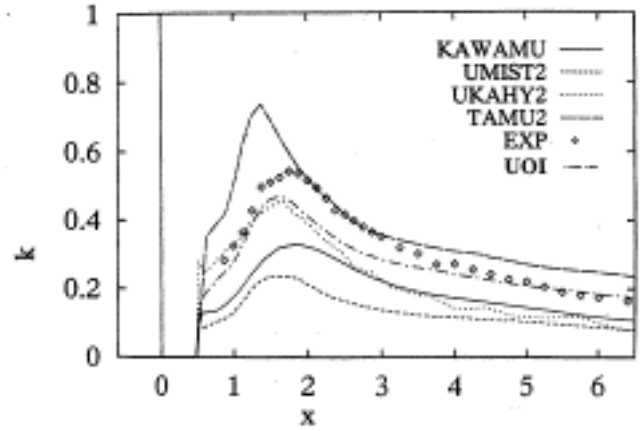

a) Total kinetic energy of fluctuations (periodic + turbulent). Results from Rottach-Egern Workshop and UOI from Grenoble Workshop

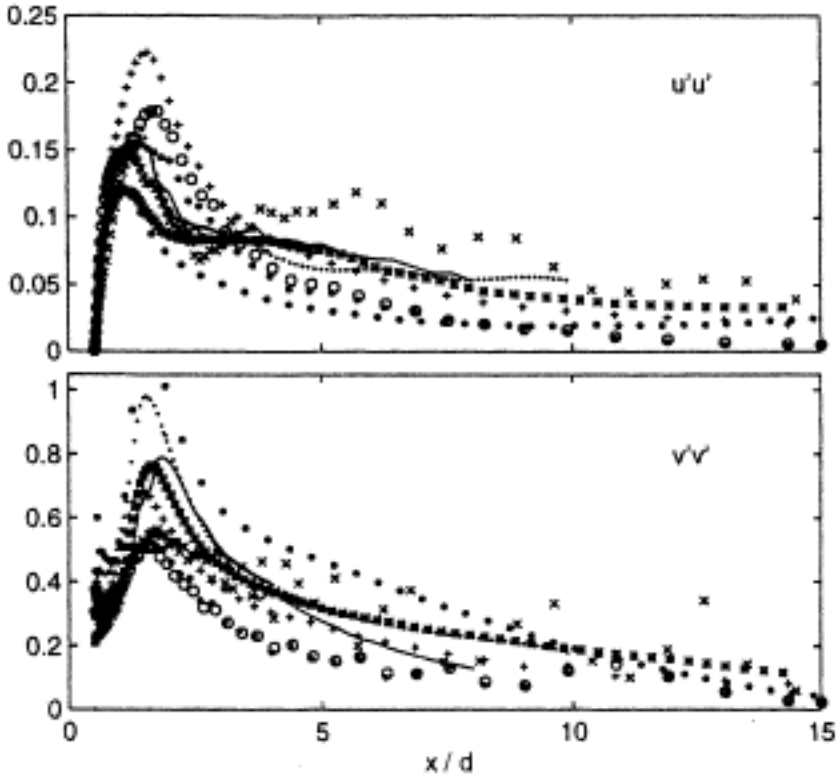

b) Total.u' and v' fluctuations (periodic + turbulent). Results from Grenoble Workshop

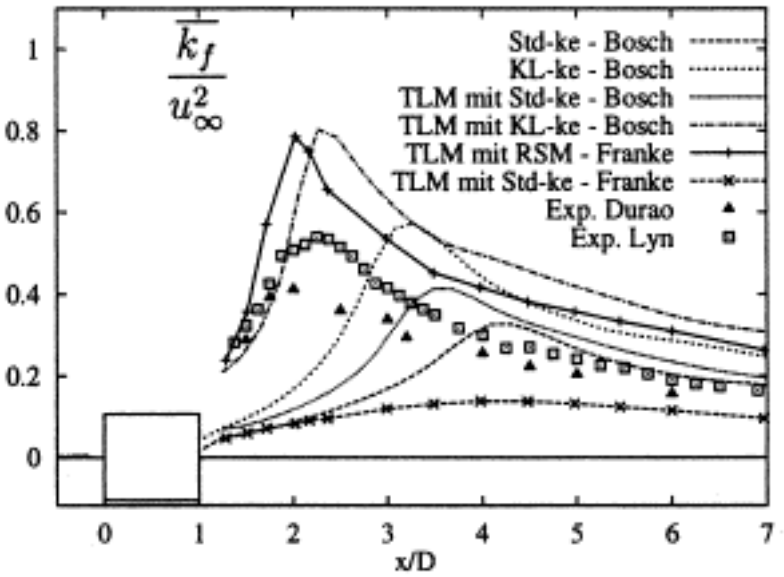

c) RANS calculations of total kinetic energy of fluctuations (periodic + turbulent) from Bosch and Rodi (1998)

Figure 4: Fluctuations along centre-line of square cylinder

RANS results for the total kinetic energy of the fluctuations are shown in Fig. 4c). Here, the total value is composed of resolved periodic fluctuations and turbulent

fluctuations stemming from the turbulence models. The standard k-ε model produces a far too low k-level. This is due to the over-production of turbulent kinetic energy in front of the cylinder, resulting in a too strong damping of the periodic shedding motion in the wake of the cylinder. When the Kato-Launder modification is applied together with the two-layer approach, k is overpredicted. This is also the case with the RSM model, but the peak is now at the correct location. It appears that shedding is overpredicted with these models.

Results of LES calculations for the distribution of mean-pressure along the cylinder walls are presented in Schmidt (2000) and Giammanco et al. (2001) where they are compared with experimental results of Bearman and Obasaju (1982). Although the Reynolds number is different (Re = 10.000) in these experiments, the agreement is quite reasonable; the largest descrepancies are found along the side-wall underneath the flapping shear-layers.

Further results of LES calculations, mainly distributions of mean velocity and components of the fluctuations along the cylinder centre-line can be found in Védy and Voke (2001). The conclusions of their systematic study will be reported in the best practice advice section that follows.

Best Practice Advice for the UFR

Key Physics

The most important feature of the flow past a long, square cylinder is the unsteady, alternate shedding of vortices from the cylinder which are swept downstream forming a Karman vortex street that dominates the wake. The fluctuations due to the shed vortices have a dominant frequency and cause a strong momentum exchange. The first advice is that this unsteady vortex-shedding flow cannot be calculated by steady RANS calculations, but as a minimum unsteady 2D RANS must be used. The shed vortices are mainly two-dimensional, but large-scale 3D structures modulate the shedding frequency and the amplitude of fluctuations. The approach flow is largely inviscid with very thin laminar layers on the front side. The flow separates at the front corners and thin flapping separated shear layers form along the sides with a thin reverse flow region having large gradients. These shear layers are first laminar, but then undergo transition to turbulence after about 15% of the side length. In the experiment, the oncoming flow had a uniform velocity and 2-3% turbulence of an unknown length scale.

Numerical issues

As mentioned already, an unsteady calculation procedure must be used also for RANS calculations. First order upwind schemes for the convection terms cannot be used as they introduce too much numerical diffusion, damping out the unsteady vortex motion. Even higher order upwind schemes were found to be problematic in LES calculations and hence central differencing should be used. the minimum grids in the cross sectional plane (see Fig.1) are as follows:

- RANS with wall-functions ≈ 100 x 70
- Two-layer RANS ≈ 170 x 170
- LES ≈ 150 x 150

For LES this is probably still not fine enough near the side-walls where the gradients are particularly large. In the 3D LES calculations at least 20 grid-points should be used in the spanwise direction. Grid stretching in the wake should be avoided as this was found to have an adverse effect in some LES calculations (but was not confirmed by all).

Computational domain and boundary conditions

The lateral boundaries should be placed at the location of the walls of the water tunnel, so that the blockage is the same as in the experiment. This means that the lateral width of the domain should be 14 cylinder widths D, as shown in Fig. 1. At the lateral boundaries, slip conditions (symmetry conditions) can be used. The inflow plane, where uniform conditions are applied, should be placed about 10 D upstream of the cylinder as it was found that at x/D ≈ -5 used in many calculations there is already an influence of the cylinder on the oncoming flow. In RANS calculations the turbulence level at inflow should be equal to the experimental level of 3% and the turbulence length scale should be chosen such that the ratio of eddy-viscosity to molecular viscosity is about 10 rather than a significantly higher value. In all LES carried out so far, turbulence at the inflow was neglected. The outflow plane should be placed at least 15 D downstream of the cylinder and here zero gradient conditions can be used in RANS calculations and the convective conditions should be used in LES calculations. The wall boundary conditions are discussed in the section on physical modelling. In LES calculations the spanwise extent of the domain should be at least 4 D and periodicity conditions should be applied at the boundaries.

Physical modelling

The standard k - ε RANS model with wall-functions should not be used for this flow as it produces rather poor results because the periodic motion is strongly underpredicted. This is to a large extent due to the excessive turbulence production in the stagnation flow resulting from the use of this model. The Kato-Launder modification removes this problem and yields improved results, but together with wall-functions these are still not very good and hence wall functions should be avoided in RANS calculations. The excessive turbulence production problem is also absent when a RSM model used, but this overpredicts the periodic motion — however more testing with this model is really needed. When combined with the two-layer approach resolving the near-wall region, the Kato-Launder version of the k - ε model yields reasonable results for engineering parameters such as the Strouhal number, the mean drag coefficient and the size of the mean recirculation zone. The fluctuating quantities are not reliably predicted by this model. In particular, the turbulent stochastic fluctuations are severely underpredicted in the RANS calculations. The fairly high values of these fluctuations in

the experiment (see Rodi, 1997, 2002) most likely stem from low frequency variations of the shedding motion due to 3D effects which cannot be accounted for in 2D RANS calculations. LES allows to pick up these motions and in general gives a better simulation of the details of the flow and is hence more suitable. In fact, the more successful of the LES predictions are better than any of the RANS calculations reported. Hence, if the details of the flow are of interest, LES should be used rather than RANS. However, the price to be paid is a large increase in computing time, roughly 10 fold if one goes from a RANS calculation with two-layer approach to a LES calculation and 36 fold if one goes from a RANS calculation with wall-functions to an LES (Rodi, 2002).

The subgrid-scale model used in LES was found not to be crucial for this flow; the standard Smagorinsky model, with wall-damping functions, is adequate for this application. Also, there was no significant influence of the near-wall treatment detected, i.e. whether a no-slip condition or wall-functions were used, but the advice is to use a no-slip condition if a sufficiently fine near-wall resolution can be afforded. The quality of an LES calculation depends in the end mainly on the calculation domain, which needs to be chosen sufficiently large, and on a sufficiently fine resolution.

Application uncertainties

The main uncertainty concerns the turbulence of the oncoming flow. The intensity was measured 3D upstream of the cylinder, but no information is available from the experiment on the length scale and hence considerable uncertainties exist about the characteristics of the turbulence at the inflow boundary when this is placed 10 D upstream of the cylinder as recommended. If the inflow boundary is moved closer to the cylinder, then uncertainties are introduced concerning the mean velocity and pressure at this boundary.

Recommendations for future work

The unsteady RANS calculations have all been done with fairly dated turbulence models and it would be interesting to learn about the performance of modern models like the Spalart-Allmaras model, the Menter SST model or Durbin's V2F model for this flow. It was further found that even the most successful LES simulations are not entirely satisfactory as they had difficulties to get both the near-wake region and the recovery in the further downstream region predicted correctly. Hence, also further LES test calculations are recommended. Of particular interest would be calculations with a spanwise extent of the calculation domain larger than 4D. Also, the inflow boundary should be placed further upstream of the cylinder, at about 10D (so far the inflow boundary was placed around 5D upstream). Further, an even better numerical resolution should be attempted, especially near the side walls. Finally, the turbulence in the oncoming free stream was neglected so far and should be included in the inflow conditions. Additional experiments would also be helpful in which the turbulence at inflow is carefully measured and for different Reynolds numbers and free stream turbulence levels to allow a wider testing of the calculation procedures.

References

Agard Advisory Report 345 (1998): A selection of test cases for the validation of large-eddy simulations of turbulent flows. This includes a CD containing the data.

Bearman, P. and Obajasu (1982): An experimental study of the pressure fluctuations on fixed and oscillating square-section cylinders, *J. Fluid Mech.*, **119**, pp. 297-321.

Bosch, G. and Rodi, W. (1998): Simulation of vortex shedding past a square cylinder with different turbulence models, *Int. J. Numer. Meth. Fluids*, **28**, pp. 601-616.

Cantwell, B. and Coles, D. (1983): An experimental study of entrainment and transport in the turbulent near wake of a circular cylinder, *J. Fluid Mech.*, **136**, pp. 321-374.

Germano, M., Piomelli, U., Moin, P., Cabot, W.H. (1991): A dynamic subgrid-scale eddy-viscosity model, *Physics of Fluids A.*, **3**, pp 1760-1765.

Giammanco, R., Simons, E., Benocci, C. (2001): Large-eddy simulation of turbulent flows over a cylinder of square cross-section, in: Direct and Large-Eddy Simulation — IV, B.J. Guerts et al. (eds.), pp. 337-344, Kluwer Academic Publishers.

Kato, M. and Launder, B.E. (1993): The modelling of turbulent flow around stationary and vibrating square cylinders, *Proc. 9th Symp. Turbulent Shear Flows*, Kyoto, p.10-4-1.

Lakehal, D., Thiele, S., Duchamp, D., Lageneste, L. Buffat, M. (1998). Computation of vortex-shedding flows past a square cylinder employing LES and RANS, in: Notes on Numerical Fluid Mechanics, Numerical Flow Simulation I, E.H. Hirschel (ed.), **66**, Vieweg Verlag, pp. 260-277.

Lyn, D.A. and Rodi, W. (1994): The flapping shear layer formed by flow separation from a forward corner of a square cylinder, *J. Fluid Mech.*, **267**, pp. 253-276.

Lyn, D.A., Einav, S., Rodi, W., and Park, J.H. (1995): A laser Doppler velocimeter study on ensemble-averaged characteristics of the turbulent near-wake of a square cylinder, *J. Fluid Mech.*, **304**, pp. 285-319.

Martinuzzi, R.J., and Wu, K.C.Q. (1997): An experimental investigation of the flow around a two-dimensional square prism in the proximity of a solid wall: effect of the gap size, *Proc. 11th Symposium on Turbulent Shear Flows*, Grenoble, France, pp. 11.16-11.23.

Rodi, W. (1997): Comparison of LES and RANS calculations of the flow around bluff bodies, *J. of Wind Engineering and Industrial Aerodynamics*, **69-71**, pp. 55-75.

Rodi, W., Ferziger, H.J., Breuer, M., Pourquie, M. (1995): Proc. Workshop on Large-Eddy Simulation of Flows Past Bluff Bodies, Rottach-Egern, Germany, June 1995.

Rodi, W., Ferziger, H.J., Breuer, M., Pourquie, M. (1997): Status of Large-Eddy Simulation: Results of a Workshop, *J. Fluid Eng.*, **119**, pp. 248-262.

Rodi, W. (2002). Large-eddy simulation of the flow past bluff bodies, in: Strategies for Turbulent and Transitional Flows, B.E. Launder and N. Sandham (eds.), Cambridge University Press, pp. 361-391.

Schmidt, S. (2000): Grobstruktursimulation turbulenter Strömungen in komplexen Geometrien und bei hohen Reynoldszahlen, Ph.D. thesis, Technical University of Berlin.

Schmidt, S. and Thiele, S. (2002): Comparison of numerical methods applied to the flow over wall-mounted cubes, *Int. J. of Heat and Fluid Flow*, **23**, pp. 330-339.

Sohankar, A., Davidson, L., Norberg, C. (2000): Large eddy simulation of flow past a square cylinder: comparison of different subgrid-scale models, *J. Fluid Eng.*, **122**, pp. 39-47.

Védy, E. and Voke, P.R. (2001): Large-eddy simulations of the flow past a square cylinder, Report FRC/2001.04, University of Surrey, UK.

Voke, P.R. (1997): Flow past a square cylinder: Test case LES2, in: Direct and Large-Eddy Simulation II, J.P. Chollet et al. (eds.), ERCOFTAC Series, Vol. 5, Kluwer Academic Publishers, pp. 355-373.

Warner, H. and Wengle, H. (1989): Large-eddy simulation of the flow over a square rib in a channel, *Proc. 7th Symp. Turbulent Shear Flows*, Stanford University, pp. 10.2.1-10.

Zdravkovich, M. (1997): *Flow Around Circular Cylinders*, Vol. 1, Fundamentals, Oxford University Press.

Zhu, J. (991). A low-diffusive and oscillation-free convection scheme, *Comm. Appl. Numer. Methods*, **7**, pp. 225-232.